Kraft Lignin/Poly(ethylene oxide) Blends: Effect of Lignin Structure on Miscibility and Hydrogen Bonding

Satoshi Kubo, John F. Kadla

Biomaterials Chemistry, Department of Wood Science, The University of British Columbia, Vancouver, British Columbia, Canada V6T 1Z4

Received 25 August 2003; accepted 2 February 2005
DOI 10.1002/app.22245
Published online in Wiley InterScience (www.interscience.wiley.com).

ABSTRACT: Blends of poly(ethylene oxide) (PEO) with softwood kraft lignin (SKL) were prepared by thermal blending. The miscibility behavior and hydrogen bonding of the blends were investigated by differential scanning calorimetry (DSC) and Fourier transform infrared (FTIR) spectroscopy. The experimental results indicate that PEO was miscible with SKL, as shown by the existence of a single glass-transition temperature over the entire composition range by DSC. In addition, a negative polymer–polymer interaction energy density was calculated on the basis of the melting point depression of PEO. The formation of strong intermolecular hydrogen bonding was detected by FTIR analysis. A comparison of the results obtained for the SKL/PEO blend system with those previously observed for a hardwood kraft lignin/PEO system revealed the existence of stronger hydrogen bonding within the SKL/PEO blends but weaker overall intermolecular interactions between components; this suggested that more than just hydrogen bonding was involved in the determination of the blend behavior in the kraft lignin/PEO blends. © 2005 Wiley Periodicals, Inc. J Appl Polym Sci 98: 1437–1444, 2005

Key words: biopolymers; blends; differential scanning calorimetry (DSC); infrared spectroscopy; miscibility

INTRODUCTION

Lignin is a readily available and relatively inexpensive natural polymer. It is an amorphous polyaromatic polyol that serves many functions in wood. Commercially, lignin is obtained as a byproduct of wood-free papermaking. The limited market for lignin,[1] less than 2% of the total available lignin, has favored its utilization as a fuel source. However, as a fuel, it is very inefficient, producing less than one-fourth of the energy per pound as middle distillate (diesel, jet, and boiler) fuels. Nonetheless, lignin combustion plays a critical role in the chemical recovery process of papermaking, and it is vital to this industry.

Today, an ever-increasing number of paper mills are becoming chemical-recovery limited; if paper production is to be maximized, the byproduct lignin can no longer be used in its traditional role as a fuel. In addition to the traditional lignin-based products, where lignin is used in the formulation of dispersants, adhesives, surfactants, and stabilizers (antioxidants) for plastics and rubber,[2] lignin-based thermoplastics[3,4] and advanced composites[5] are receiving increasing attention. Lignin has been used in plastic materials since the 1930s;[6] however, the incorporation of various monomers or polymers into the lignin structure results in properties unsuitable for structural materials.[7] Glasser and coworkers[8,9] showed that through the manipulation of the network structure and substituents in lignin, the physical properties of lignin-based materials can be manipulated. They found that the noted brittleness of lignin, caused by the globular structure of lignin fragments, could be abolished by the incorporation of a variety of polyether components in the network structure. That is, a decrease in the glass-transition temperatures (T_g's) and brittleness could be achieved through the introduction of soft molecular segments capable of a plastic response to mechanical deformation.

Recently, we reported the production of lignin-based carbon fibers from commercial lignin.[10] Although continuous thermal spinning of lignin-based fibers was achieved without any chemical modification of the lignin, the resulting lignin fibers were very brittle. Processability and brittleness were improved through polymer blending. The spinning properties of the lignin-based polyblends were strongly dependent on the physical and thermal properties of the blended polymer, specifically the solubility parameter, melt viscosity, and thermal decomposition temperature.[4] Fiber morphology was also affected by the nature of the blending polymer, and a unique core–shell morphology was obtained in certain immiscible blends.[10]

In two hardwood kraft lignin (HKL)-based polyblends, one miscible [poly(ethylene oxide) (PEO)/HKL[11]] and one immiscible [poly(vinyl alcohol)/

Correspondence to: J. F. Kadla (john.kadla@ubc.ca).
Contract grant sponsor: Canada Research Chair Program.

TABLE I
Chemical Properties of Isolated Lignins

	Functional group *(mmol/g)*				Molecular mass	
	Hydroxyl					
Sample	Aliphatic	Aromatic	Biphenol	Methoxyl	M_w	Dispersity
SKL	5.6	3.8	2.1	4.2	2800	2.0
HKL	4.1	4.3	1.1	5.9	2400	1.8

M_w = weight-average molecular weight.

HKL[12]], the presence of strong specific intermolecular interactions, that is, hydrogen bonding, was detected. Fourier transform infrared (FTIR) spectroscopy and differential scanning calorimetry (DSC) analysis revealed that phenolic hydroxyl groups formed stronger hydrogen bonds with PEO than aliphatic hydroxyl groups. With lignin model compounds, it was shown that the hydrogen bonding between PEO and 2,2′-dihydroxyl-3,3′-dimethoxyl-biphenyl, a prevalent biphenolic structure in lignin, was stronger than that of other phenolic lignin moieties.

Softwood lignins contain substantially more biphenolic structures than hardwood lignins.[13] Therefore, the intermolecular interactions between PEO and softwood lignins should be different than that of hardwood lignins. In this article, a commercial softwood kraft lignin (SKL) was thermally blended with PEO with the same process as that used previously for the HKL/PEO system. The resulting polyblends were analyzed by DSC and FTIR, and the effect of lignin structure on the blend miscibility and polymer–polymer interactions is discussed.

EXPERIMENTAL

Materials

SKL was obtained from Westvaco Corp. (Charleston, SC). The lignin was repeatedly washed with dilute HCl (Aldrich Chemicals, Oakville, ON, Canada) to exchange sodium counterions, vacuum-dried over P_2O_5, and recovered as a fine powder. The chemical properties of the lignin are listed in Table I. PEO with a viscosity-average molecular weight of 100,000 was purchased from Union Carbide Corp. (Houston, TX) and was used as received.

Lignin characterization

Density values were determined according to ASTM D 70-97 with a multivolume pycnometer 1305 (Micromeritics, Norcross, GA). Elemental analysis of the lignin samples was carried out at E & R Microanalytical Laboratories, Inc. (New York). Methoxyl content was determined according to the modified procedure of Viebock and Schwappach.[14] Aliphatic and aromatic hydroxyl contents were determined with ^{31}P-NMR and ^{1}H-NMR. Quantification of ^{1}H-NMR was obtained from the integration ratios of aliphatic and aromatic acetoxy protons of the acetylated lignin preparations relative to the internal standard *p*-nitrobenzaldehyde.

The relative average molecular mass and molecular mass distribution of the acetylated lignin samples were determined by gel permeation chromatography (Waters Associates ultraviolet (UV) and refractive index (RI) detectors) with styragel columns at 50°C and with tetrahydrofuran as the eluting solvent. The gel permeation chromatography system was calibrated with standard polystyrene samples. The injection volume was 100 μL, and the acetylated lignin concentration was 1 mg/mL of tetrahydrofuran.

The lignin preparations were acetylated by the dissolution of 200 mg of lignin in 10 mL of pyridine/acetic anhydride (1 : 1 v/v) and reacted for 48 h at room temperature. The solution was poured over crushed ice and filtered. The resulting precipitate was then washed with cold water/HCl, dried, and subjected to a second acetylation treatment.

Thermal blending

The lignin was thermally treated before blending at 160°C *in vacuo* for 30 min to remove volatile contaminants.[15] Blends of various PEO/lignin ratios were prepared by mechanical mixing followed by thermal extrusion with an Atlas Laboratory Mixing Extruder (Atlas Corp., Chicago, IL). The resulting pellet sample was transformed into fiber with the same extruder equipped with a 1/32-in. (ca. 0.8 mm) spinneret.

Characterization of the SKL/PEO blends

Thermal properties of lignin and its PEO blends were characterized with a TA Instruments Q100 DSC instrument (New Castle, DE) at a scanning rate of 20°C/min over the temperature range −90 to 200°C. The measurements were made with 5.0- to 5.5-mg samples under a nitrogen atmosphere. T_g was recorded as the midpoint temperature of the heat capacity transition of the second heating run. Samples were run in duplicate and are reported as the average of the two runs

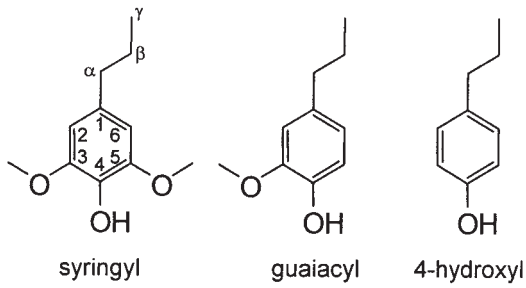

Figure 1 Fundamental structure of a molar unit of lignin.

and were within experimental error of each other (±1.0°C).

The equilibrium melting point (T_m^0) was determined with Hoffman–Weeks plots.[16] In a typical experiment, 5.0-mg samples, as weight fractions of PEO, were heated to 90°C and maintained at this temperature for 10 min to completely eliminate PEO crystallinity. The samples were than quenched to the desired isothermal crystallization temperature (T_{ic}) and held at that temperature for 2 h to allow complete crystallization. The melting temperature after isothermal crystallization (T_m') was measured at a heating rate of 10°C/min; T_m' was determined as the peak top temperature.

The FTIR spectra of the polymer blends were determined with the diffuse-reflectance Fourier transform infrared (DR-FTIR) method (because of the physical properties of the polymer blends, it was difficult to prepare uniform KBr pellets for FTIR analysis with transmittance detection). The polymer blends (10 mg) were dispersed in KBr (200 mg), and DR-FTIR measurements were recorded on a PerkinElmer 16PG FTIR spectrometer (Boston, MA); 256 scans were collected with a spectral resolution of 4.0 cm^{-1}. Because of the hygroscopic nature of the polymer blends, a pure nitrogen flow was maintained over the sample during collection.

RESULTS AND DISCUSSION

Lignin characterization

Lignin biosynthesis involves the dehydrogenative polymerization of three primary monolignols: *p*-coumaryl alcohol, coniferyl alcohol, and sinapyl alcohol.[17] As a result, the structure of lignin is very much dependent on the wood species and the processing conditions used in its isolation. Figure 1 shows representative aromatic units found in lignin. Table I shows the chemical and functional group analysis of the SKL and HKL. The total phenolic hydroxyl group content of the SKL, 3.8 mmol/g, was close to that of the HKL, 4.3 mmol/g. However, as expected, the SKL did not contain any syringyl structures and had a larger number of guaiacyl hydroxyl groups. The SKL also contained a substantially larger amount of biphenol, dimeric guaiacyl structures commonly referred to as 5-5′ biphenyl units, and *p*-hydroxylphenyl structures.[13] It is known that the thermal properties of lignin are related to its aromatic ring structure,[15] as are its hydrogen-bonding properties.[11] Thus, the difference in the types of phenolic hydroxyl groups between the SKL and HKL should have profoundly affected the thermal and hydrogen-bonding properties of the corresponding PEO blends.

Blend preparation

Unlike that of the HKL fibers, the thermal spinning of the SKL fibers was problematic. It has been reported that the thermal molecular motion of softwood lignin is inferior to that of HKL due to its highly condensed structures.[15] As shown in Table I, the SKL had a large amount of condensed linkages (5-5′-biphenyl units). However, at temperatures greater than 250°C, the SKL could be transformed into a rubbery material. Unfortunately, the molten viscosity of the SKL melt appeared to be very high and was not suitable for fiber spinning. Moreover, thermal decomposition of the SKL took place at this temperature (Fig. 2).

Polymer blending with PEO substantially improved the thermal processability of the SKL. The thermal blending and fiber spinning temperatures for the SKL/PEO blends are listed in Table II. Although good fiber spinning was achieved for all of the blend compositions investigated, more than 50% PEO was required to achieve continuous fiber spinning with high take-up speeds.

Blend miscibility: thermal analysis

DSC has been extensively used to investigate miscibility in polymer blends. A single compositional-dependent T_g is an indication of full miscibility at a dimensional scale between 5 and 15 nm.[18] Figure 3 shows the DSC analyses of SKL/PEO blends of various compo-

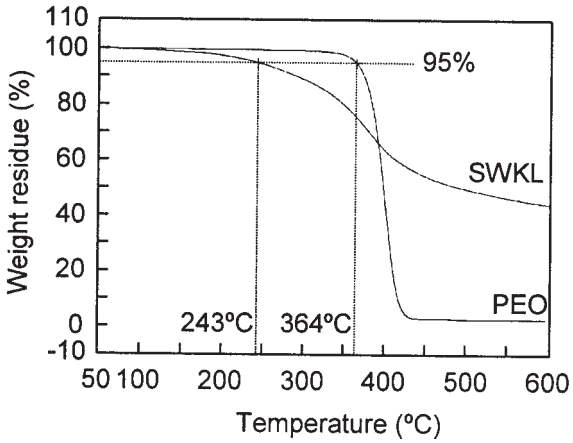

Figure 2 TGA curves of SKL and PEO.

TABLE II
Blending and Spinning Temperatures of the SKL/PEO Blends

Weight fraction (w/w)		Blending temperature	Spinning temperature
SKL	PEO	(°C)	(°C)
1	0	248–250	x
0.875	0.125	240–241	x
0.75	0.25	233–235	x
0.625[a]	0.375[a]	234	219–224
0.50	0.50	240	238–240
0.375	0.625	233–234	224–225
0.25	0.75	218–236	234–235
0.125	0.875	230–236	234–236
0	1	—	216–222

x = fibers could not be continuously spun.
[a] The winding speed of this blend fiber was slower than that of the other blend fibers.

sitions. The pure amorphous SKL exhibited one T_g at 155°C, substantially higher than that observed for HKL (106°C).[11] This difference in T_g could have been due to the chain flexibility of the lignin molecules. The observed T_g decreased in temperature with increasing PEO blend content. Similarly, the melting temperature (T_m) of the PEO component in the blends decreased with increasing lignin content. Table III summarizes the thermal properties of PEO, SKL, and the corresponding polymer blends.

Because of the high crystallinity of PEO, the apparent change in heat flow of PEO at the glass transition was much lower than that of SKL, 0.11 versus 0.39 J g^{-1} °C^{-1}, respectively. Increasing the incorporation of SKL resulted in a decrease in the crystallinity of the PEO fraction; at greater than 50% SKL, no PEO melting peak was observed. This was similar to the results obtained for HKL/PEO blends.[11] The decrease in PEO crystallinity was slightly faster in the SKL/PEO blends than in the HKL/PEO (Fig. 4), although the fiber spinning of SKL-rich blends was difficult. These results indicate that the SKL was mixed favorably with PEO.

The detection of a single T_g via thermal analysis provided important information as to the composition of the individual amorphous phases present in the material. The single T_g strongly suggested that these were fully miscible blends with a homogeneous amorphous phase. In general, the formation of miscible binary polymer blends depends on the occurrence of exothermic interactions between the two components being mixed.[19] The manner in which T_g varies with blend composition is reflective of the relative strengths of these intermolecular interactions. Figure 5 shows the compositional dependence on the T_g of the SKL/PEO blend system. A negative deviation from a simple weighted average was observed. This result indicates that there were relatively weak favorable interactions between the blend components.[20]

Several theoretical and empirical equations have been proposed for the prediction of T_g in miscible polymer blends.[20—24] One of the most comprehensive was that derived by Lu and Weiss.[20] With enthalpy as the thermodynamic variable and with no adjustable parameters, a general expression for the glass-transition temperature of a binary polymer mixture (T_{gm}) in terms of the T_g's of the individual components and the nature of the interactions between the components was derived. The Lu and Weiss equation is as follows:

$$T_{gm} = \frac{(w_1 T_{g1} + k w_2 T_{g2})}{(w_1 + k w_2)} + \frac{A w_1 w_2}{(w_1 + k w_2)(w_1 + b w_2)(w_1 + c w_2)^2} \quad (1)$$

$$A = \frac{-\chi R (T_{g1} - T_{g2}) c}{M_1 \Delta c_{p1}} \qquad k = \frac{\Delta c_{p2} - w_1 \delta c_p^1}{\Delta c_{p1} - w_2 \delta c_p^g} \quad (2)$$

where $b = M_2/M_1$ (where M_i is the molar mass per chain segment of polymer i), $c = \rho_1/\rho_2$ (where ρ_i is the density of polymer i), w_i is the weight fraction of polymer i, δc_{pi} is the specific heat change due to mixing, and $\Delta c_{pi} = c_{pi}^l - c_{pi}^g$ at the change in the specific heat of polymer i (T_{gi}), and the superscripts g and l denote the glassy and liquid states, respectively. Thus, the T_g composition behavior of binary blends is governed by the parameters k and A, where A is linearly dependent on thermodynamic interaction parameter (χ).

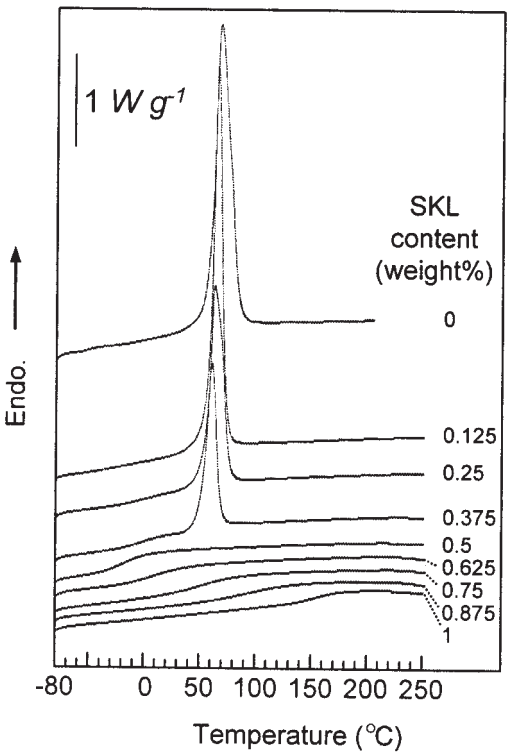

Figure 3 DSC curves of the SKL/PEO blends.

TABLE III
DSC Results for the Lignin/PEO Blend Fiber

Weight fraction (w/w)						Weight fraction in the amorphous phase (w/w)	
SKL	PEO	T_g (°C)	ΔC_p (J g^{-1} °C^{-1})	T_m (°C)	ΔH (J/g^{-1})	Lignin	PEO
1	0	155	0.39	x	0	1	0
0.875	0.125	90	0.54	x	0	0.875	0.125
0.75	0.25	50	0.63	x	0	0.75	0.25
0.625	0.375	9	0.61	x	0	0.625	0.375
0.50	0.50	−19	0.54	x	0	0.50	0.50
0.375	0.625	−1	0.38	60	62	0.56	0.44
0.25	0.75	−2	0.29	62	97	0.52	0.48
0.125	0.875	−29	0.10	65	125	0.37	0.63
0	1	−50	0.11	67	168	0	1

x = these values could not be detected. ΔH = heat of fusion.

In polymer blends characterized by weak specific intermolecular interactions between the miscible polymer blend components, the effect of k is greater than A,[20] and the equation is simplified to the Gordon–Taylor equation:[21]

$$T_{gm} = \frac{(w_1 T_{g1} + k' w_2 T_{g2})}{(w_1 + k' w_2)} \quad (3)$$

where $k' = k + A/(T_{g2} - 1)$. Here, k' can be used qualitatively as a measure of the intermolecular interactions in the polymer blend. In systems with strong specific polymer–polymer interactions, such as hydrogen bonding, T_{gm} may be quantified by Kwei's equation:[23]

$$T_{gm} = \frac{(w_1 T_{g1} + k w_2 T_{g2})}{(w_1 + k w_2)} + A' w_1 w_2 \quad (4)$$

where $k = \Delta c_{p2}/\Delta c_{p1}$. In this case, A' may be regarded as a measure of the interactions between the polymer components. Table IV lists the various equations and fitting parameters for the SKL/PEO blend system.

The Kwei[23] and Gordon–Taylor[21] equations fit the experimental data well (Fig. 5). A k' of 0.27 (R^2 = 0.990) was obtained from the nonlinear least-squares best-fit of the Gordon–Taylor equation. This value was slightly lower than that for the HKL/PEO blend system[11] [k' = 0.37 (R^2 = 0.982)], indicating that the intermolecular interaction of SKL with PEO was slightly weaker than that of HKL. Similarly, the calculated value of A' from the Kwei equation (A' = −269) was lower than that for the HKL/PEO blend system (A' = −170). (As the fitting curve for the Kwei equation does not show any inflection or extreme points, the value of k can be taken as unity.[25]) This indicated a lower propensity to form intermolecular interactions in the SKL/PEO blend system than in the HKL/PEO system.[11]

The observed T_g phenomenon, which was related to segmental motions in the polymer, was also affected by steric hindrance and variations in the flexibility of the polymer chains.[23,25] As a result, A' was related to both hydrogen-bond formation and changes in the environment of the polymer chains. The flexibility of

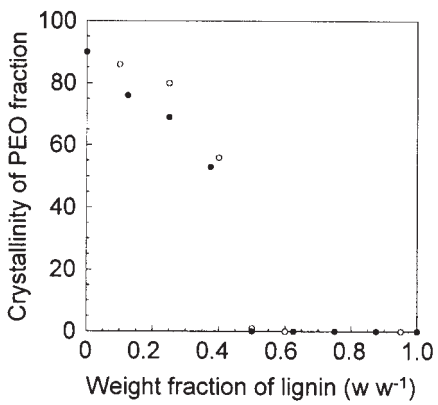

Figure 4 Change in the crystallinity of the PEO fraction in the lignin/PEO blend fiber: (●) SKL/PEO and (○) HKL/PEO.

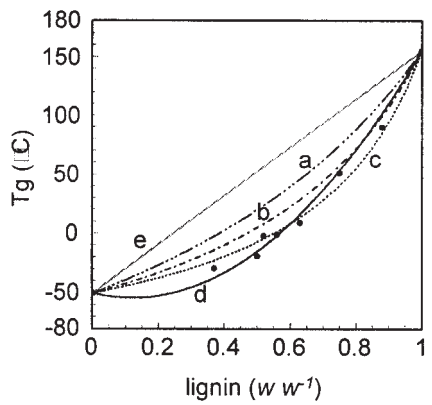

Figure 5 Composition dependence on T_g of the lignin/PEO blend: (a) Fox, (b) Couchman, (c) Gordon–Taylor, (d) Kwei, and (e) linear additive lines.

TABLE IV
Parameters Estimated from the T_g Variation Curves of the Lignin/PEO Blends

Equation	Parameter
Fox: $\frac{1}{T_g} = \frac{w_1}{T_{g1}} + \frac{w_2}{T_{g2}}$	— ($R^2 = 0.812$)
Couchman: $\ln T_g = \frac{w_1\Delta C_{p1}\ln T_{g1} + w_2\Delta C_{p2}\ln T_{g2}}{w_1\Delta C_{p1} + w_2\Delta C_{p2}}$	— ($R^2 = 0.950$)
Gordon–Taylor: $T_g = \frac{w_1 T_{g1} + k' w_2 T_{g2}}{w_1 + k' w_2}$	$k' = 0.27$ ($R^2 = 0.990$)
Kwei: $T_g = \frac{w_1 T_{g1} + k w_2 T_{g2}}{w_1 + k w_2} + A w_1 w_2$	$A = -269$ $k = 1$ ($R^2 = 0.990$)

HKL molecules were higher than that of SKL molecules, as the T_g of HKL was lower than that of SKL. However, the propensity to form stronger intermolecular interactions with PEO, that is, hydrogen bonding, should have been greater for SKL due to the larger amount of 5-5′-biphenol moieties, although the calculated A' value was lower in the SKL/PEO blend system than in the HKL/PEO system.

Melting point depression (Δt_m)

The ΔT_m of a crystalline polymer blended with an amorphous polymer provides important information about the blend's miscibility and its associated polymer–polymer interaction parameter (χ). The reduction in temperature is caused by a thermodynamic depression arising from a reduction in chemical potential due to the presence of the polymeric solvent. When two polymers are miscible in the molten state, the chemical potential of the crystallizable polymer decreases due to the addition of the second component. This leads to a reduction in T_m^0 with increasing amorphous polymer content, especially in blends containing specific interactions between components. An immiscible blend will typically not show a depression of T_m^0.

T_m^0 is typically determined with the Hoffman–Weeks approach.[16] Figure 6 presents the Hoffman–Weeks plot and ΔT_m as a function of the volume fraction of SKL for the SKL/PEO blends. In Figure 6(A), the experimental results are fit with $T_m' = \phi T_{ic} + (1 - \phi)T_m^0$,[16,26] where ϕ is a stability parameter and T_{ic} is the isothermal crystallization temperature. The values of T_m^0 for PEO and its blends with SKL were obtained by an extrapolation procedure with a least-squares fit of the data to the intersection with $T_m' = T_{ic}$. However, as discussed and demonstrated by many groups,[27–29] the errors associated with the Hoffman–Weeks approach can be significant, and a small uncertainty in T_m can profoundly affect the value of χ. In certain blends, the appearance of a ΔT_m may in fact be the result of incomplete crystallization rather than thermodynamic considerations. This is particularly the case in polymer blend systems with very small ΔT_m's. However, we previously found that in lignin/PEO systems, T_m was independent of the crystallization period, provided the crystallization period was longer than 2 h.[11] As listed in Table V, ϕ was approximately 0.12 for the various compositions of the SKL/PEO blends. This result indicates that morphological effects may no longer have been significant in the case of the SKL/PEO blends, as ϕ depended on crystalline size and perfection. Moreover, a large ΔT_m, 7.0°C, was determined (Table V).

With the equation of Nishi and Wang,[26] which is based on the Flory–Huggins theory,[19] ΔT_m is given by the following equation:[19,26]

$$\frac{1}{V_1}\left[\frac{1}{T^0_{m-blend}} - \frac{1}{T^0_{m-PEO}}\right] = -\frac{BV_{2u}\ V_1}{\Delta H_{2u} T^0_{m-blend}} \qquad (5)$$

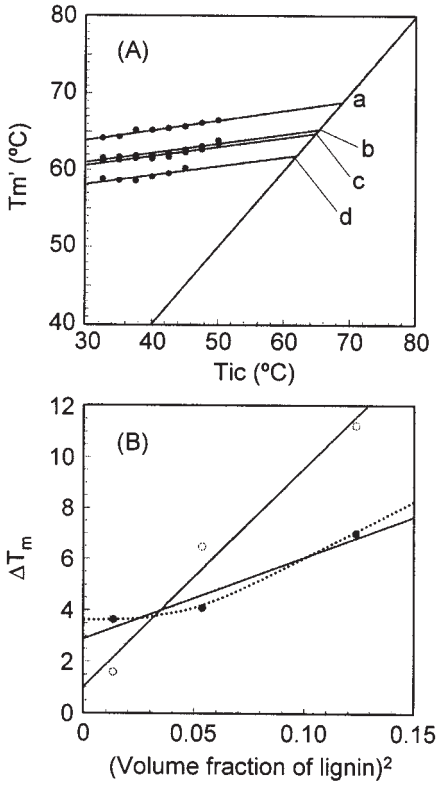

Figure 6 ΔT_m of the PEO fraction in the lignin/PEO blend: (A) Hoffman–Weeks plot for the lignin/PEO blend [(a) 0/100, (b) 12.5/87.5, (c) 37.5/62.5, and (d) 25/75] and (B) ΔT_m as a function of the square of the volume fraction of lignin [ΔT_m was determined (●) from the Hoffman–Weeks plot and (○) from T_m in Table III].

TABLE V
T_m^0 and ϕ as Estimated by the Hoffman-Weeks Approach

Lignin/PEO (w/w)	T_m^0 (°C)	ϕ[a]
37.5/62.5	61.9	0.118
25/75	65.3	0.121
12.5/87.5	64.8	0.122
0/100	68.9	0.129

[a] ϕ was calculated by $T_m^0 - T_m = \phi(T_m^0 - T_c)$, where T_m* and T_c are the observed melting point and crystallization temperature, respectively.

where the subscripts 1 and 2 represent the amorphous and the crystalline polymers, respectively; V_u is the molar volume of the repeating units; ΔH_u is the heat of fusion per mole of repeat unit; R is the gas constant and B is the interaction energy density characteristic of the polymer pair and is, in practice, related to the thermodynamic interaction parameter (χ_{12}) by $B = RT_m^0$ (χ_{12}/V_{1u}). If we assumed that B or χ was composition-independent, a plot of ΔT_m versus the square of the volume fraction of lignin [Fig. 4(B) solid circles] produced a B value of -4.8 cal/cm^3, which was slightly smaller than that for the HKL/PEO blend system (-5.5 cal/cm^{-3}).[11] The sign and magnitude of the B value indicated a miscible blend with strong interactions between the blend components. However, the T_m^0 depression curve [Fig. 4(B)] deviated slightly from a linear line. Although this has been observed in other blend systems,[30,31] the nonlinearity may have been due to the composition dependence of χ. Therefore, χ values were not calculated for this system. Nonetheless, a ΔT_m was clearly observed and indicated that the intermolecular interactions between the SKL and PEO were slightly lower than the interactions in the HKL/PEO system. These results were in good agreement with the T_g observations discussed previously.

Hydrogen-bonding properties of the SKL/PEO blends

FTIR analysis of the ν_{OH} region of SKL and the blends with PEO is shown in Figure 7. The SKL fiber consisted of a broad band envelope over a range of 3600–3100 cm^{-1}. There was clear evidence of intramolecular hydrogen bonding of hydroxyl groups (3520 cm^{-1}) and/or dimeric formation via intermolecular hydrogen bonding (3420 cm^{-1}).[11] A weak shoulder at approximately 3300 cm^{-1} may have originated from multiple intermolecular hydrogen bondings of aliphatic hydroxyl groups and/or between aliphatic hydroxyl groups and condensed guaiacyl hydroxyl units (e.g., biphenol moieties).[11]

Thermally blending the SKL with PEO deformed the band shape of the ν_{OH} region. This band deformation indicated a change in the hydrogen-bonding system. New hydrogen bonds were being formed between the hydroxyl groups in SKL and the ether groups in PEO. The intensity of the broad band centered at the high wave-number region (3520 cm^{-1}) was significantly decreased by the addition of a small amount of PEO. Conversely, a new band center appeared at almost the same position as the weak shoulder of the original SKL fiber (3300 cm^{-1}). Increasing the PEO content to greater than 37.5% produced a new broad band centered at about 3134 cm^{-1}. This large change in the hydroxyl group stretching region was consistent with that observed for the HKL/PEO blend system [Fig. 7(B)].[11] However, the shift in the broad hydroxyl group stretching band region was larger in the SKL/PEO system [Fig. 7(A) vs Fig. 7(B)]. In our previous report,[11] the FTIR spectrum of a biphenol lignin model compound and PEO bend showed band centers at 3226 and 3146 cm^{-1}, which were assigned to intermolecular hydrogen bonding between biphenols and between biphenol and PEO, respectively. The 3146 cm^{-1} wave-number band was close to the broad band center observed for the SKL/PEO blend. Thus, biphenol was likely a key structure in the formation of strong hydrogen bonds in the SKL/PEO blend system.

It was evident that SKL formed stronger hydrogen bonds with PEO than HKL. However, thermal analy-

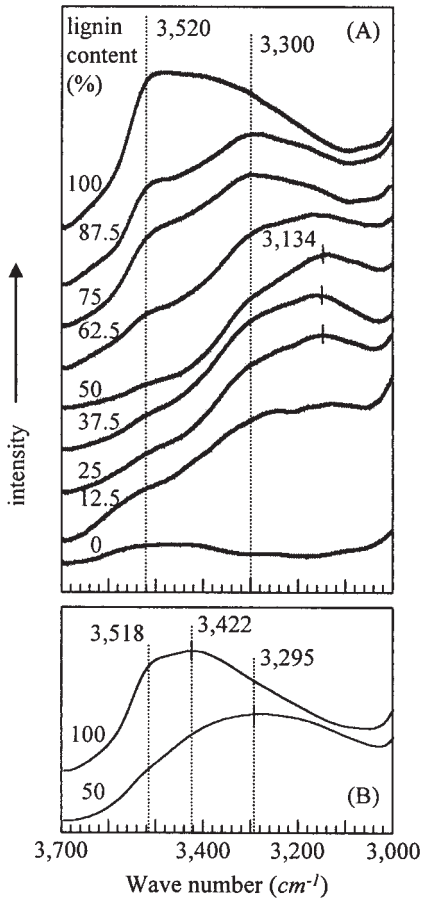

Figure 7 DR-FTIR spectra of the lignin/PEO blend fibers in the ν_{OH} region: (A) SKL/PEO and (B) HKL/PEO blends.[7]

sis showed that the strength of the interaction (B_{SKL} = −4.8 cal/cm^3 vs B_{HKL} = − 5.5 cal/cm^3) and the propensity to interact (A_{SKL}' = −269 vs A_{HKL}' = −170) with PEO was stronger for HKL than SKL. Hydrogen bonding was not the only factor impacting the lignin/PEO blend stability; differences in macromolecular structure must have played an important role.

Pronounced noncovalent and non-hydrogen-bonding attractive interactions between individual molecular kraft lignin species have been reported;[32] these supramacromolecular complexes are responsible for the cohesiveness of kraft-lignin-based materials. In kraft-lignin-based polyblends, compatibility is facilitated by the ability of the blending component to dismantle these supramacromolecular complexes.[11] In the lignin/PEO blend systems, the individual HKL components are structurally less rigid and more thermally mobile than SKL components. SKL had a higher T_g than HKL, and although the SKL was transformed into a rubbery material by the heating, it did not exhibit thermal flow. In lignin, high thermal flexibility allowed the lignin molecules to dissociate from each other, enabling good mixing with PEO. During this process, hydrogen bonds were formed between the lignin and PEO. As lignin formed stronger hydrogen bonds with PEO than with other lignin molecules, hydrogen bonding was likely a key factor in blend formation. However, our results indicate that hydrogen bonding was not the only factor impacting blend formation and blend stability; dispersion of each molecule in the blend must have also been an important factor. Thus, the ability of PEO to disrupt these attractive interactions within the supramacromolecular complexes of lignin was not only affected by the strength of the specific interactions between PEO and kraft lignin and the number or extent of interaction between components but also the magnitude of the noncovalent attractive interactions between the individual molecular kraft lignin species.

CONCLUSIONS

Lignin-based thermoplastic blends were produced with a commercial SKL and PEO. DSC analysis of the thermally blended polymers indicated miscible blend behavior over the blend ratio studied. As with HKL/PEO blends, a negative deviation of T_g from the weight-average values was observed; indicating weak favorable interchain interactions between SKL and PEO. FTIR analysis revealed the formation of strong intermolecular hydrogen bonding between the blend components. A comparison with HKL/PEO blends showed that stronger intermolecular hydrogen bonds were formed in the SKL/PEO blends, which was likely the result of the large amount of biphenol units in SKL (~35%) compared to that in HKL (~20%). However, the thermal analysis data revealed the extent and strength of the interaction were lower for the SKL/PEO system than the corresponding HKL system. Although the biphenol structures formed strong hydrogen bonds with PEO, they also restricted the thermal mobility of the lignin macromolecule. Thus, the effect of PEO incorporation on the blend T_g may have depended on more than just hydrogen bonding and may have been more influenced by the strong intramolecular and intermolecular interactions existing within the lignin macromolecule and supramolecular complexes.

References

1. Fengel, D.; Wegener, G. Wood: Chemistry, Ultrastructure, Reactions; de Gruyter: Berlin, 1984.
2. Glasser, W. G.; Northey, R. A.; Schultz, T. P. Lignin: Historical, Biological, and Materials Perspectives; American Chemical Society: Washington, DC, 2000.
3. Li, Y.; Mlynar, J.; Sarkanen, S. J Polym Sci Part B: Polym Phys 1997, 35, 1899.
4. Kubo, S.; Gilbert, R. D.; Kadla, J. F. In Natural Fibers, Biopolymers and Their Biocomposites; Drzal, L. T., Ed.; CRC: Boca Raton, FL, 2005; pp 671–698.
5. Kadla, J. F.; Kubo, S.; Venditti, R. A.; Gilbert, R. D.; Compere, A. L.; Griffith, W. Carbon 2002, 40, 2913.
6. Esselen, G. J.; Bacon, F. S. Ind Eng Chem 1938, 30, 125.
7. Glasser, W. G.; Sarkanen, S. Lignin: Properties and Materials; American Chemical Society: Washington, DC, 1989.
8. Glasser, W. G.; Barnett, C. A.; Rials, T. G.; Saraf, V. P. J Appl Polym Sci 1984, 29, 1815.
9. Glasser, W. G.; Jain, R. K. Holzforschung 1993, 47, 225.
10. Kadla, J. F.; Kubo, S.; Venditti, R. A.; Gilbert, R. D. J Appl Polym Sci 2002, 85, 1353.
11. Kadla, J. F.; Kubo, S. Macromolecules 2003, 36, 7803.
12. Kubo, S.; Kadla, J. F. Biomacromolecules 2003, 4, 561.
13. Adler, E. Wood Sci Technol 1977, 11, 169.
14. Chen, C.-L. In Methods in Lignin Chemistry; Dence, C. W., Ed.; Springer-Verlag: Berlin, 1992; p 301.
15. Kubo, S.; Ishikawa, N.; Uraki, Y.; Sano, Y. Mokuzai Gakkaishi 1997, 43, 655.
16. Hoffman, J. D.; Weeks, J. J. J Chem Phys 1962, 37, 1723.
17. Sederoff, R. R.; Chang, H.-M. In Wood Structure and Composition; Goldstein, I. S., Ed.; Marcel Dekker: New York, 1991; pp xiv, 488.
18. Paul, D. R.; Bucknall, C. B. Polymer Blends; Wiley: New York, 2000.
19. Flory, P. J. Principles of Polymer Chemistry; Cornell University Press: Ithaca, NY, 1953.
20. Lu, X.; Weiss, R. A. Macromolecules 1992, 25, 3242.
21. Gordon, M.; Taylor, J. S. J Appl Chem 1952, 2, 493.
22. Fox, T. G. B. Am Phys Soc 1956, 1, 123.
23. Kwei, T. K.; Pearce, E. M.; Pennacchia, J. R.; Charton, M. Macromolecules 1987, 20, 1174.
24. Couchman, P. R. Macromolecules 1978, 11, 1156.
25. Lin, A. A.; Kwei, T. K.; Reiser, A. Macromolecules 1989, 22, 4112.
26. Nishi, T.; Wang, T. T.; Kwei, T. K. Macromolecules 1975, 8, 227.
27. Jo, W. H.; Lee, S. C. Macromolecules 1990, 23, 2261.
28. Cheung, Y. W.; Stein, R. S.; Chu, B.; Wu, G. W. Macromolecules 1994, 27, 3589.
29. Jonza, J. M.; Porter, R. S. Macromolecules 1986, 19, 1946.
30. Cheung, Y. W.; Stein, R. S. Macromolecules 1994, 27, 2512.
31. Painter, P. C.; Shenoy, S. L.; Bhagwagar, D. E.; Fishburn, J.; Coleman, M. M. Macromolecules 1991, 24, 5623.
32. Li, Y.; Sarkanen, S. Macromolecules 2002, 35, 9707.